Advances in Computer, Signals and Systems (2024)
Clausius Scientific Press, Canada

DOI: 10.23977/acss.2024.080706
ISSN 2371-8838 Vol. 8 Num. 7

Dynamic Model Establishment and Simplification for 4WID-4WIS Electric Vehicles

Hao Zhu[1], Su Zhou[2,3,*], Xin Gu[2,4]

[1]*Shanghai Motor Vehicle Inspection Certification & Tech Innovation Center Co., Ltd, Shanghai, 201805, China*
[2]*Tongji University, Shanghai, 201804, China*
[3]*Shanghai Zhongqiao Vocational and Technical University, Shanghai, 201514, China*
[4]*Shanghai New Power Automotive Technology CO., LTD, Shanghai, 200438, China*
[*]*Corresponding author: suzhou@tongji.edu.cn*

Keywords: Four-wheel independent drive; four-wheel independent steering; dynamic model; Pacejka magic tire formula; simplified model

Abstract: Based on the Pacejka magic tire formula, this paper establishes a nonlinear full model of a four-wheel independent drive and four-wheel independent steering car. Using the discrete step method, the paper solves the nonlinear implicit differential equations, simplifies the model, and determines its applicable scope. Finally, the paper compares the simulation results of three simplified models with those of the full model. The results show that under the corresponding applicable conditions, the results of the simplified models are very similar to those of the full model, allowing the full model to be replaced by the simplified model.

1. Introduction

The four-wheel independent drive and four-wheel independent steering (4WID-4WIS) electric vehicle has consistently been a focal point in automotive industry research. Each wheel is equipped with a hub motor that provides driving torque and a steering mechanism for adjusting the steering angle, resulting in excellent maneuverability and a wide variety of driving modes. The vehicle dynamics characteristics, with eight degrees of freedom, make the 4WID-4WIS vehicle control model fundamentally different from traditional four-wheel vehicle models. Common tire formulas used in vehicle dynamics include the Dugoff tire model, Pacejka tire model and etc. Among them, the Pacejka magic tire formula [1] uses trigonometric function combinations to fit tire characteristics. When the lateral acceleration is less than 0.4g and the yaw angle is less than 5 degrees, the Pacejka tire formula achieves extremely high fitting accuracy. The robustness of the Pacejka magic tire formula and the high confidence in the results it produces are reasons for its widespread use in the automotive industry and its adoption in this paper.

The research on related control issues of 4WIS-4WID vehicles is extensive. Solea R, Filipescu A et al. [2] used sliding mode control to track and control the trajectory of car based on 4WIS vehicle model. Maoqi et al.[3] studied the maneuverability of 4WS vehicles equipped with wheel hub motors. Shi et al. [4] proposed a double-layer dynamic decoupling control system based on the 2-DOF model

of 4WS vehicles, addressing the issue of vehicle yaw instability. Chen et al. [5] studied the trajectory tracking problem of 4WIS-4WID vehicles and derived a control model based on the 2-DOF model. Liang et al.[6] combined active steering and direct yaw moment control to resolve the challenges of lateral control in 4WID-4WIS vehicles at high speeds. Liu et al.[7] proposed a fault-tolerant control method that improved the trajectory tracking performance and stability of 4WID-4WID vehicles.

The dynamics of 4WIS-4WID vehicles have also been extensively studied by many scholars. Peng Hang et al.[8] established a nonlinear dynamic model for 4WIS based on the Dugoff tire model and transformed the nonlinear model into a linear model for MPC control. Fahimi[9] conducted control research on 4WS vehicle, establishing a 6-DOF (degrees of freedom) vehicle model based on the Pacejka tire model, and then simplifying it to a 3-DOF nonlinear model. Iervolino et al.[10] established a nonlinear vehicle full model based on the Pacejka tire model. Hang et al. [11], in order to study the stability control algorithm for 4WID-4WIS vehicles, simplified the vehicle model to a 2-DOF model by ignoring pitch and roll motions. These studies have provided valuable insights and tools for understanding and controlling the complex dynamics of 4WIS-4WID vehicles.

This paper aims to establish a nonlinear dynamic model suitable for 4WID-4WIS vehicles based on the Pacejka magic tire formula model, propose an algorithm solution process applicable to this model, and construct a full-model solution. Under different conditions, the full model is simplified, and the solution space of the simplified model is finally obtained. Additionally, this paper compares the differences between the simplified model and the full model.

2. 4WID-4WIS Dynamic vehicle model

Figure 1 illustrates the relevant variables of a 4WID-4WIS vehicle in both the inertial and vehicle coordinate systems. In the diagram, u, v represents the velocities of the centroid along the longitudinal and lateral directions of the vehicle body, respectively; γ is the yaw rate of centroid, and β is the yaw angle. $u_i, v_i (i = fl, fr, rl, rr)$ represent the velocities of tire centers along the longitudinal and lateral directions of the vehicle body, respectively; $u_{wi}, v_{wi} (i = fl, fr, rl, rr)$ represent the tire velocities along the longitudinal and lateral directions in the tire coordinate system, respectively. F_{ui}, F_{vi} are the forces acting on the wheels along the longitudinal and lateral directions of the vehicle body; F_{wxi}, F_{wyi} are the forces acting on the wheels along the longitudinal and lateral directions in the tire coordinate system, respectively; δ_i represents the steering angle of each wheel.

As shown in Figure 1, the relationship between the speeds and displacements in the vehicle coordinate system and those in the X and Y directions of the inertial coordinate system can be expressed by Equation (1). Here, v_X and v_Y represent the velocities of the centroid in the x and y directions; X and Y represent the displacements of the centroid in the x and y directions. Considering vehicle dynamics, for 4 tires labeled as $i = fl, fr, rl, rr$, the forces acting on the tires from the ground are expressed as shown in Equation (2).

$$\begin{cases} v_X = u\cos\beta - v\sin\beta \\ v_Y = u\sin\beta + v\cos\beta \\ X = \int v_X dt \\ Y = \int v_Y dt \\ \beta = \int v dt \end{cases} \tag{1}$$

$$\begin{cases} F_{ui} = F_{wxi}\cos\delta_i - F_{wyi}\sin\delta_i \\ F_{vi} = F_{wxi}\sin\delta_i + F_{wyi}\cos\delta_i \\ M_{fl} = -0.5 \cdot F_{ufl} \cdot B_f + F_{vfl} \cdot L_f \\ M_{fr} = 0.5 \cdot F_{ufr} \cdot B_f + F_{vfr} \cdot L_f \\ M_{rl} = -0.5 \cdot F_{url} \cdot B_r - F_{vrl} \cdot L_r \\ M_{rr} = 0.5 \cdot F_{urr} \cdot B_r - F_{vrr} \cdot L_r \end{cases} \tag{2}$$

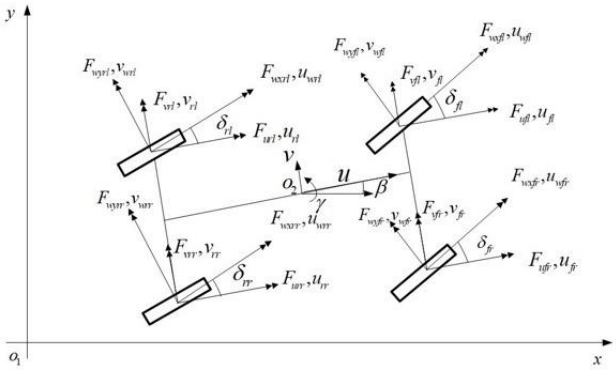

Figure 1: Schematic Diagram of 4WID-4WIS Vehicle Forces

According to Newton's third law, we derive Equation (3). In this equation, a_u and a_v represent the longitudinal and lateral accelerations of the centroid; M_i is the torque exerted by the wheels on the centroid ; F_w is the wind resistance acting on the vehicle body; m is the fully loaded mass of the vehicle; B_f and B_r are the front and rear wheelbase; L_f and L_r are the distances from the centroid to the front and rear axles; J_z is the inertia moment of the entire vehicle around the centroid; C_D is the drag coefficient; A is the vehicle lateral area; and ρ is the air density.

$$\begin{cases} ma_u = m(\dot{u} - v\gamma) = \sum F_{ui} - F_w - F_f \\ ma_v = m(\dot{v} + u\gamma) = \sum F_{vi} \\ J_z\dot{\gamma} = \sum M_i \\ F_w = C_D A\rho u^2/2 \\ F_f = fG \end{cases} \tag{3}$$

The relationship between input forces on tires of each wheel labeled as $i = fl, fr, rl, rr$ and the reactive forces exerted by the ground on the tires is represented by Equation (4). In Equation (4), ω_i represents the rotational angular velocity of the wheel, T_{di} represents the input torque of the wheel, r_{wi} represents the rolling radius of the wheel, and J_i represents the inertia moment of the wheel.

$$J_i\dot{\omega}_i = T_{di} - F_{wxi} \cdot r_{wi} \tag{4}$$

When considering influence of centroid acceleration on the vertical load of vehcle wheels. F_{zi} is the vertical load on wheel, L is the wheelbase of the vehicle, and h_{cg} is the height of vehicle's centroid.

The relationship between the vehicle's centroid speed and tire speed derived from the vehicle coordinate system is expressed in Equation (6). In this equation, u, v represent the component of the vehicle's centroid speed along the vehicle coordinate system, and γ represents the yaw rate of the centroid.

Based on the results derived from Equation (6), the paper can further deduce the longitudinal speed, lateral speed, and tire sideslip angle in the tire coordinate system. In Equation (7), u_{wi} represents the longitudinal velocity component of the current tire, v_{wi} represents the lateral velocity component of the current tire, and α_{wi} represents the tire sideslip angle.

$$\begin{cases} F_{zfl} = \dfrac{mgL_r}{2L} - \dfrac{ma_u h_{cg}}{2L} - \dfrac{ma_v L_r h_{cg}}{LB_f} \\ F_{zfr} = \dfrac{mgL_r}{2L} - \dfrac{ma_u h_{cg}}{2L} + \dfrac{ma_v L_r h_{cg}}{LB_f} \\ F_{zrl} = \dfrac{mgL_f}{2L} + \dfrac{ma_u h_{cg}}{2L} - \dfrac{ma_v L_f h_{cg}}{LB_r} \\ F_{zrr} = \dfrac{mgL_f}{2L} + \dfrac{ma_u h_{cg}}{2L} - \dfrac{ma_v L_f h_{cg}}{LB_r} \end{cases} \tag{5}$$

$$\begin{cases} u_{fl} = u - \gamma \cdot B_f/2 \,, v_{fl} = v + \gamma \cdot L_f; \\ u_{fr} = u + \gamma \cdot B_f/2 \,, v_{fr} = v + \gamma \cdot L_f; \\ u_{rl} = u - \gamma \cdot B_r/2 \,, v_{rl} = v - \gamma \cdot L_r; \\ u_{rl} = u + \gamma \cdot B_r/2 \,, v_{rl} = v - \gamma \cdot L_r; \end{cases} \tag{6}$$

$$\begin{cases} u_{wi} = u_i cos\delta_i + v_i sin\delta_i \\ v_{wi} = -u_i sin\delta_i + v_i cos\delta \\ \alpha_{wi} = arctan(v_{wi}/u_{wi}) \end{cases} \tag{7}$$

Based on the longitudinal speed in the tire coordinate system, the tire slip ratio of the current vehicle can be derived in Equation (8):

$$\kappa = \begin{cases} \dfrac{\omega_i r_\omega - u_{\omega i}}{u_{\omega i}} \; ; \;\; \omega_i r_\omega - u_{\omega i} < u_{\omega i} \\ \dfrac{\omega_i r_\omega - u_{\omega i}}{\omega_i r_\omega} \; ; \;\; \omega_i r_\omega - u_{\omega i} > u_{\omega i} \end{cases} \tag{8}$$

The magic tire model is used to calculate the longitudinal and lateral forces of a tire. The expression for the longitudinal force is as shown in Equation (9-11):

$$F_x = F_{x_0} \cdot G_{x\alpha} \tag{9}$$

$$\begin{cases} F_{x_0} = (D_x sin(C_x arctan(B_x x_1 - E_x(B_x x_1 - arctan(B_x x_1))))) \\ x_1 = \kappa \\ C_x = B_0 \\ D_x = B_1 F_z + B_2 F_z \\ BCD_x = (B_3 F_z + B_4 F_z) e^{-B_5 F_z} \\ B_x = BCD_x/(C_x \times D_x) \\ E_x = B_6 F_z + B_7 F_z + B_8 \end{cases} \tag{10}$$

$$\begin{cases} G_{x\alpha} = G_{x\alpha_1}/G_{x\alpha_0} \\ G_{x\alpha_1} = cos(C_{\alpha s} arctan(B_{\alpha x}.\alpha_s - E_{\alpha x}(B_{\alpha x}.\alpha_s - arctan(B_{\alpha x}.\alpha_s)))) \\ G_{x\alpha_0} = cos(C_{\alpha s} arctan(B_{\alpha x}.\alpha_H - E_{\alpha x}(B_{\alpha x}.\alpha_H - arctan(B_{\alpha x}.\alpha_H)))) \\ C_{\alpha s} = b_0 \\ B_{\alpha x} = b_1 cos(arctan(b_2 \kappa)) \\ \alpha_H = b_3 \\ \alpha_3 = -|\alpha| + \alpha_H \\ E_{\alpha x} = b_4 + b_5 F_z \end{cases} \tag{11}$$

The expression for the longitudinal force is as shown in Equation (12-14):

$$F_y = F_{y_0} \cdot G_{y\kappa} \tag{12}$$

$$\begin{cases} F_{y_0} = (D_y sin(C_y arctan(B_y x_y - E_y(B_y x_y - arctan(B_y x_y))))) \\ x_y = \alpha \\ C_y = A_0 \\ D_y = A_1 F_z + A_2 F_z \\ BCD_y = A_3 sin(A_4 arctan(A_5 F_z)) \\ B_y = BCD_y/(C_y \times D_y) \\ E_y = (A_6 F_z + A_7)(1 + A_8 sign(\alpha)) \end{cases} \tag{13}$$

$$\begin{cases} G_{y\kappa} = G_{y\kappa_1}/G_{y\kappa_0} \\ G_{y\kappa_1} = cos(C_{y\kappa} arctan(B_{y\kappa}.\kappa_s - E_{y\kappa}(B_{yk}.\kappa_s - arctan(B_{y\kappa}.\kappa_s)))) \\ G_{y\kappa_0} = \cos\,(C_{y\kappa} \arctan\,(B_{y\kappa}.\kappa_{Hyk} - \cdots \\ E_{y\kappa}(B_{yk}.\kappa_{Hyk} - arctan(B_{y\kappa}.\kappa_{Hyk})))) \\ C_{y\kappa} = a_0 \\ B_{y\kappa} = a_1 cos(arctan(a_2(\alpha - a_3))) \\ E_{y\kappa} = a_4 + a_5 F_z \\ \kappa_s = \kappa + \kappa_{Hyk} \\ \kappa_{Hyk} = a_6 + a_7 F_z \end{cases} \tag{14}$$

3. Establishment and Solution of Differential Equation Models

Based on the previously mentioned dynamic model of driving, the state variables, intermediate variables, and control variables are defined as shown in Equations (15-17).

$$X = [x, y, \Psi, V_X, V_Y, \Upsilon, \omega_{fl}, \omega_{fr}, \omega_{rl}, w_{rr}] \tag{15}$$

$$I = [F_X, F_Y, M, F_{txfl}, F_{txfr}, F_{txrl}, F_{txrr}] \tag{16}$$

$$U = [T_{fl}, T_{fr}, T_{rl}, T_{rr}, D_{fl}, D_{fr}, D_{rl}, D_{rr}] \tag{17}$$

In these equations, x and y represent the coordinates of the vehicle's centroid in the inertial coordinate system, Ψ denotes the yaw angle of the centroid, V_X and V_Y are the velocity components of the centroid in the inertial coordinate system, γ is the yaw rate of the centroid, and $\omega_{fl}, \omega_{fr}, \omega_{rl}, \omega_{rr}$ represent the four wheels rotational speeds of the vehicle. T and D stand for tire torque and tire angle, respectively. $F_X, F_Y,$ and M represent the forces acting on the vehicle's centroid, while $F_{txfl}, F_{txfr}, F_{txrl}, F_{txrr}$ represent the longitudinal forces of the four wheels. Based on these definitions, the dynamic driving model of the vehicle can be expressed in the following form:

$$\begin{aligned} X &= F(X, I, U); \\ I &= g^{-1}(\dot{X}, X, U); \end{aligned} \tag{18}$$

The specific forms of these equations are shown in Equations (19-20):

$$\begin{cases} \dot{x} = V_X * \cos\Psi - V_Y * sin\Psi \\ \dot{y} = V_X * \sin\Psi + V_Y * cos\Psi \\ \dot{\Psi} = \gamma \\ \dot{V}_X = \dfrac{F_X - F_w - F_f}{m} + \gamma * V_Y \\ \dot{V}_Y = \dfrac{F_Y}{m} - \gamma * V_X \\ \dot{\gamma} = \dfrac{M}{J_z} \\ \dot{\omega}_{fl} = \dfrac{T_{dfl} - F_{txfl} * r_{fl}}{J_{wfl}} \\ \dot{\omega}_{fr} = \dfrac{T_{dfr} - F_{txfr} * r_{fr}}{J_{wfr}} \\ \dot{\omega}_{rl} = \dfrac{T_{drl} - F_{txrl} * r_{rl}}{J_{wrl}} \\ \dot{\omega}_{rr} = \dfrac{T_{drr} - F_{txrr} * r_{rr}}{J_{wrr}} \end{cases} \tag{19}$$

$$\begin{cases} X_1 = f_1(X_3, X_4, X_5) \\ \dot{X}_2 = f_2(X_3, X_4, X_5) \\ \dot{X}_3 = f_3(X_6) \\ \dot{X}_4 = f_4(X_4, X_5, I_1(\dot{X}_4, \dot{X}_5, X_4, X_5, X_6, X_7, X_8, X_9, X_{10}, U)) \\ \dot{X}_5 = f_5(X_4, X_6, I_2(\dot{X}_4, \dot{X}_6, X_4, X_5, X_6, X_7, X_8, X_9, X_{10}, U)) \\ \dot{X}_6 = f_6(I_3(\dot{X}_4, \dot{X}_5, X_4, X_5, X_6, X_7, X_8, X_9, X_{10}, U)) \\ \dot{X}_7 = f_7(U_1, I_4(\dot{X}_4, \dot{X}_5, X_4, X_5, X_6, X_7, U_1, U_5)) \\ \dot{X}_8 = f_8(U_2, I_5(\dot{X}_4, \dot{X}_5, X_4, X_5, X_6, X_8, U_2, U_6)) \\ \dot{X}_9 = f_9(U_3, I_6(\dot{X}_4, \dot{X}_5, X_4, X_5, X_6, X_9, U_3, U_7)) \\ \dot{X}_{10} = f_{10}(U_4, I_7(\dot{X}_4, \dot{X}_5, X_4, X_5, X_6, X_{10}, U_4, U_8)) \end{cases} \tag{20}$$

The dynamic driving model based on magic tire formula is a nonlinear implicit system of differential equations containing many trigonometric functions (Equations 18-20). Such a system

cannot be solved directly and requires numerical methods for step-by-step solutions. In this paper, a solution strategy as outlined in Table 1 is adopted. Given initial state and initial control, speeds, sideslip angles, slip ratios, and tire rotational speed change rates of each tire at current time step can be calculated first. Subsequently, vertical forces on tires and tire slip ratios can be computed. These quantities are then used in the Pacejka magic tire formula to calculate the forces acting on tires from the ground. Finally, the state variables at the next time step are computed based on the dynamic equations, and the time t is updated. Figure 2 presents the algorithm flowchart for the nonlinear model in this paper. The arrows indicate the interrelationships between the calculated quantities, with the starting point of the arrow representing the calculation condition and the endpoint representing the calculation result. For example, to calculate the longitudinal and lateral forces of the tires in the model, it is necessary to compute the vertical tire forces, wheel slip ratios, and tire sideslip angles beforehand.

Table 1: Numerical methods for step-by-step solution strategy of nonlinear model on GPU

The algorithm for solving the dynamic model based on the Pacejka magic tire formula
Inputs: initial state variables, control variables, calculation step size h, and the calculation interval [a,b] Output: state variables under the given control variables Wen t<b: Based on the initial state variables, the relevant quantities of each tire are calculated: tire speeds, sideslip angles, tire slip rates, and vertical forces. The change rate of tire rotation speed is computed based on the initial state variables and control variables. The forces acting on the current tire are calculated by substituting the tire slip rate, sideslip angle, and vertical load into the magic tire formula. The computed tire forces are then substituted into the differential equations to solve for the next state variables. The calculated state variables are used as the initial state variables for the next calculation interval.
The time variable t is updated to t=t+h.
End the calculation and return the state variables at each time step

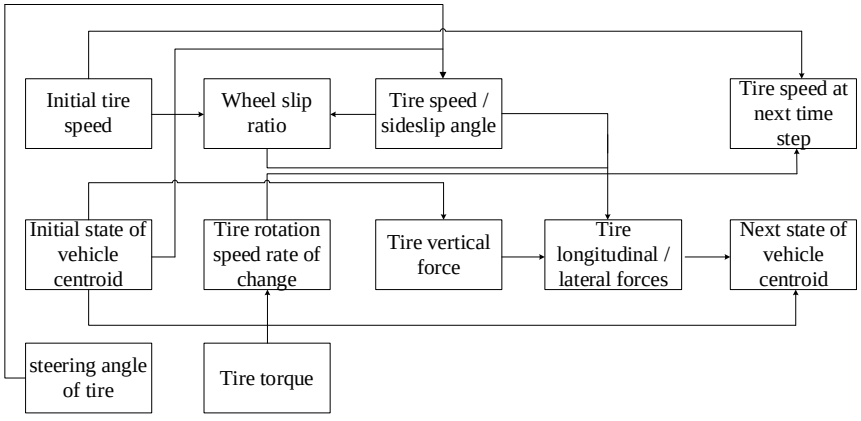

Figure 2: Algorithm flowchart for the nonlinear model distributed on GPU

4. Model Simplification

This paper adopts the strategy shown in Figure 3 to compare the solution spaces of the full model and simplified models based on the magic formula tire model. The paper primarily involves three

simplified models, including: the simplified model based on Taylor series expansion, the five-degree-of-freedom two-wheel model based on the Pacejka magic formula tire model, and the model that ignores the yaw angle.

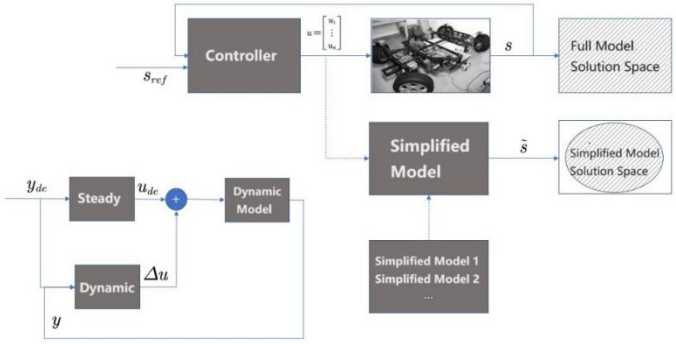

Figure 3: Comparison of the model solution space

1) The simplified model based on Taylor series expansion can transform the DAE model into ODE equations for solving.

2) The five-degree-of-freedom two-wheel model based on the Pacejka magic formula tire model can be used in most cases where the left and right wheel angles do not differ significantly.

3) In some four-wheel independently driven studies, the yaw angle is ignored. Similarly, this simplification is also demonstrated in this paper.

4.1 The simplified model based on Taylor series expansion

According to Taylor series expansion for multivariate functions, at the point $(x_k^1, x_k^2, \dots, x_k^n)$, the following equation can be derived:

$$\begin{aligned} \mathrm{f}(x^1,x^2,\cdots,x^n) &= \mathrm{f}(x_k^1,x_k^2,\cdots,x_k^n)+\dots\sum_{i=1}^{\cdot\cdot}(x^i-x_k^i)f'_{x^i}(x_k^1,x_k^2,\cdots,x_k^n)+\dots \\ \dots &\frac{1}{2!}\sum_{i,j=1}^{n}(x^i-x_k^i)(x^j-x_k^j)f''_{ij}(x_k^1,x_k^2,\cdots,x_k^n)+o^n \end{aligned} \tag{21}$$

In this paper, the strategy is adopted to solve the differential equation by expanding the intermediate variable I at the initial value of the state variable and ignoring higher-order terms. Specifically, the state variable, control variable, and intermediate variable are defined as follows:

$$\begin{gathered} X_0 = [x_0,y_0,\Psi_0,V_{x0},V_{y0},Y_0,\omega_{fl0},\omega_{fr0},w_{rl0},\omega_{rr0}] \\ U_0 = [T_{fl0},T_{fr0},T_{rl0},T_{rr0},D_{fl0},D_{fr0},D_{rl0},D_{rr0}] \\ I = I_0 + I'(X_0)\cdot(X-X_0) \end{gathered} \tag{22}$$

The intermediate variable used are:

$$\begin{gathered} F_t = [F_{txfl},F_{txfr},F_{txrl},F_{txrr},F_{tyfl},F_{tyfr},F_{tyrl},F_{tyrr}]; \\ X_1 = [\dot{V}_x,\dot{V}_y,V_x,V_y,Y,w_{fl},w_{fr},w_{rl},w_{rr},D_{fl},D_{fr},D_{rl},D_{rr},YV_y,YV_x]; \\ C_1 = [C_{xfl},C_{xfr},C_{xrl},C_{xrr},C_{yfl},C_{yfr},C_{yrl},C_{yrr}]; \\ F = [FX,FY,M]; \end{gathered} \tag{23}$$

Then, a relational expression can be derived as shown in (24).

$$\begin{gathered} F_t = B_t X_1 + C_1; \\ \mathrm{F} = A_t F_t = A_{t1}A_{t2}F_t; \end{gathered} \tag{24}$$

Finally, the intermediate quantity I can be expressed in the form of Equation (25):

$$\mathrm{I} = \begin{bmatrix} A_t \\ \sim A \end{bmatrix} F_t = \begin{bmatrix} A_t \\ \sim A \end{bmatrix} (B_t X_1 + C_1) = \begin{bmatrix} A_{t1} * A_{t2} \\ \sim A \end{bmatrix} (B_t X_1 + C_1);$$
$$\sim\mathrm{A} = \begin{bmatrix} 1 & 0 & 0 & 0 & 0 & 0 & 0 & 0 \\ 0 & 1 & 0 & 0 & 0 & 0 & 0 & 0 \\ 0 & 0 & 1 & 0 & 0 & 0 & 0 & 0 \\ 0 & 0 & 0 & 1 & 0 & 0 & 0 & 0 \end{bmatrix}; \tag{25}$$

The differential Equation (19) can be written as:

$$\begin{bmatrix} \dot{V}_x \\ \dot{V}_y \\ \dot{\Upsilon} \\ \dot{w}_{fl} \\ \dot{w}_{fr} \\ \dot{w}_{rl} \\ \dot{w}_{rr} \end{bmatrix} + \begin{bmatrix} 0 & -\frac{\Upsilon}{2} & -\frac{V_y}{2} & 0 & 0 & 0 & 0 \\ \frac{\Upsilon}{2} & 0 & \frac{V_x}{2} & 0 & 0 & 0 & 0 \\ 0 & 0 & 0 & 0 & 0 & 0 & 0 \\ 0 & 0 & 0 & 0 & 0 & 0 & 0 \\ 0 & 0 & 0 & 0 & 0 & 0 & 0 \\ 0 & 0 & 0 & 0 & 0 & 0 & 0 \\ 0 & 0 & 0 & 0 & 0 & 0 & 0 \end{bmatrix} \begin{bmatrix} V_x \\ V_y \\ \Upsilon \\ w_{fl} \\ w_{fr} \\ w_{rl} \\ w_{rr} \end{bmatrix}$$
$$+ \begin{bmatrix} -\frac{1}{m} & 0 & 0 & 0 & 0 & 0 & 0 \\ 0 & -\frac{1}{m} & 0 & 0 & 0 & 0 & 0 \\ 0 & 0 & -\frac{1}{Jz} & 0 & 0 & 0 & 0 \\ 0 & 0 & 0 & \frac{r_{fl}}{J_{wfl}} & 0 & 0 & 0 \\ 0 & 0 & 0 & 0 & \frac{r_{fr}}{J_{wfr}} & 0 & 0 \\ 0 & 0 & 0 & 0 & 0 & \frac{r_{rl}}{J_{wrl}} & 0 \\ 0 & 0 & 0 & 0 & 0 & 0 & \frac{r_{rr}}{J_{wrr}} \end{bmatrix}$$
$$* \begin{bmatrix} FX - F_\omega - \mathrm{F_f} \\ FY \\ \mathrm{M} \\ Ftxfl \\ Ftxfr \\ Ftxrl \\ Ftxrr \end{bmatrix} + \begin{bmatrix} 0 \\ 0 \\ 0 \\ -\frac{T_{dfl}}{J_{wfl}} \\ -\frac{T_{dfr}}{J_{wfr}} \\ -\frac{T_{drl}}{J_{wrl}} \\ -\frac{T_{drr}}{J_{wrr}} \end{bmatrix} = 0 \tag{26}$$

By substituting Equation (25) into Equation (26), the Differential-Algebraic Equation can be transformed into an Ordinary Differential Equation at the point (X_0). Then, the following expression can be obtained:

$$\begin{bmatrix} \dot{V}_x \\ \dot{V}_y \\ \dot{\Upsilon} \\ \dot{w}_{fl} \\ \dot{w}_{fr} \\ \dot{w}_{rl} \\ \dot{w}_{rr} \end{bmatrix} + \begin{bmatrix} \frac{C_d A \rho V_x}{m} & -\frac{\Upsilon}{2} & -\frac{V_y}{2} & 0 & 0 & 0 & 0 \\ \frac{\Upsilon}{2} & 0 & \frac{V_x}{2} & 0 & 0 & 0 & 0 \\ 0 & 0 & 0 & 0 & 0 & 0 & 0 \\ 0 & 0 & 0 & 0 & 0 & 0 & 0 \\ 0 & 0 & 0 & 0 & 0 & 0 & 0 \\ 0 & 0 & 0 & 0 & 0 & 0 & 0 \\ 0 & 0 & 0 & 0 & 0 & 0 & 0 \end{bmatrix} \begin{bmatrix} V_x \\ V_y \\ \Upsilon \\ w_{fl} \\ w_{fr} \\ w_{rl} \\ w_{rr} \end{bmatrix}$$
$$+ \begin{bmatrix} -\frac{1}{m} & 0 & 0 & 0 & 0 & 0 & 0 \\ 0 & -\frac{1}{m} & 0 & 0 & 0 & 0 & 0 \\ 0 & 0 & -\frac{1}{Jz} & 0 & 0 & 0 & 0 \\ 0 & 0 & 0 & \frac{r_{fl}}{J_{wfl}} & 0 & 0 & 0 \\ 0 & 0 & 0 & 0 & \frac{r_{fr}}{J_{wfr}} & 0 & 0 \\ 0 & 0 & 0 & 0 & 0 & \frac{r_{rl}}{J_{wrl}} & 0 \\ 0 & 0 & 0 & 0 & 0 & 0 & \frac{r_{rr}}{J_{wrr}} \end{bmatrix}$$
$$* \begin{bmatrix} A1 * A2 \\ \sim A \end{bmatrix} (B_t X_1 + C_1) + \begin{bmatrix} 0 \\ 0 \\ 0 \\ -\frac{T_{dfl}}{J_{wfl}} \\ -\frac{T_{dfr}}{J_{wfr}} \\ -\frac{T_{drl}}{J_{wrl}} \\ -\frac{T_{drr}}{J_{wrr}} \end{bmatrix} = 0 \tag{27}$$

Finally, the state equation is simplified to the following form:

$$X = AX + BU + \mathrm{C}; \tag{28}$$

Since the simplified model ignores higher-order terms after expansion, it has a certain applicable range. For ε within the range (X_0, X),the error between the actual value and expanded value of I can be denoted as:

$$R_n = |I - (I_0 + I'(X_0) * (X - X_0))| = \frac{1}{2}|I''(\varepsilon)|(X - X_0)^2; \tag{29}$$

Given the upper limit of the error η,then:

$$R_n = \frac{1}{2}|I''(\varepsilon)|(X - X_0)^2 \leq \eta; \tag{30}$$

If the step $h = (X - X_0)$, it can be concluded that:

$$|I''(\varepsilon)| \leq \frac{2\eta}{h^2}; \tag{31}$$

From the above equation, it is easy to know when the second derivative of the intermediate quantity is greater than this value $2\eta/h\text{^}2$, the results calculated from the simplified equation will exceed the upper limit of the error. In this case, the simplified model can no longer be used, and the full model should be employed for the solution.

4.2 The five-degree-of-freedom two-wheel model

Considering that under certain four-wheel steering conditions, the difference between yaw angles of the left and right wheels is not significant, the yaw angles of the left and right wheels can be set as:

$$\delta_l \approx \delta_r \tag{32}$$

In this situation, the model can be converted into a five-degree-of-freedom two-wheel independently driven model, and the differential equation can be written as:

$$\begin{gathered}
\dot{x} = V_x * \cos\Psi - V_y * sin\Psi \\
\dot{y} = V_x * \sin\Psi + V_y * cos\Psi \\
\dot{\Psi} = \gamma \\
\dot{V}_x = \frac{F_X - F_w - F_f}{m} + \gamma * V_y \\
\dot{V}_y = \frac{F_Y}{m} - \gamma * V_x \\
\dot{\gamma} = \frac{M}{J_z} \\
\dot{\omega}_f = \frac{T_{df} - F_{txf} * r_f}{J_{wf}} \\
\dot{\omega}_r = \frac{T_{dr} - F_{txr} * r_r}{J_{wr}}
\end{gathered} \tag{33}$$

4.3 The Model Ignoring Yaw Angle of Centroid

In the research of path planning or control for 4WID-4WIS vehicles[12], the yaw angle of the centroid is often ignored due to its small influence. Under such conditions:

$$\begin{aligned} \beta &\approx 0 \\ \dot{x} &= v\cos\varphi \\ \dot{y} &= v\sin\varphi \end{aligned} \tag{34}$$

5. Simulation results and discussion

5.1 Presentation of Related Parameters

All the vehicle parameters in this paper are derived from the Austrian Research Promotion Agency (FFG) funded "RoboCar" project. The main parameters are shown in Table 2. Among them, L_f is the distance from the vehicle's centroid to the front axle, L_r is the distance from the vehicle's centroid to the rear axle, J_z is the moment of inertia around the z-axis, C_D is the drag coefficient, h_{cg} is the height of the centroid, r_w is the rolling radius of the tire, and J_{wi} is the moment of inertia of the tire.

Table 2: Vehicle Parameters

L[m]	L_f[m]	L_r[m]	B_f[m]	B_r[m]	M[kg]	J_z[kg.m^2]
1.29	43.9024	-1080	-53095	2	0.1418	0.1659
Cd	A[m^2]	ρ[kg/ m^2]	g[m/s^2]	H_{cg}[m]	R_w[m]	J_{wi}[kg. m^2]
1.1	6.38	7.95	-0.06	0.1	-0.18	0.0059

5.2 Simulation results

(1) Comparison of the Solution Spaces between the Full Model and the Taylor Expansion Model

In the experiments conducted in this paper, the motor power of each wheel hub was set at 1kW, and the desired torque was set at 10Nm. The calculation step of the full model was set to 0.005s. Initially, the vehicle was set to drive straight until it reached a stable state, and then a step input was given to the tire angles. A total of four experiments were performed, with the tire angles set to [5, 5, 0, 0], [0, 0, -5, -5], [5, 5, -5, -5], and [5, 10, -4, -11], respectively.

The simulation results comparing the Taylor series expansion model and the full model are shown in Figure 4. As can be seen from Figures 4(a) to 4(c), under the first three types of control, the solutions based on the Taylor series expansion model almost overlap with those of the full model. In such cases, the results calculated by the two models are consistent, and the results from the simplified model can be used to replace those of the original model. However, as illustrated in Figure 4(d), when a yaw angle control of [5, 10, -4, -11] is applied to the vehicle, the results calculated by the simplified model do not align with the full model. Specifically, the final trajectory of the simplified model deviates by approximately 5m to 7m in the x-direction, and the yaw rate and centroid speed derived from the simplified model are smaller than those of the full model. Additionally, the centroid yaw angle obtained from the Taylor series expansion model tends to be larger than those of the full model and results in significant oscillations in the calculation. The final simulation result of the simplified model is not fully satisfactory; under this control scenario, the simplified model exhibits significant deviations and is no longer suitable for solving the problem.

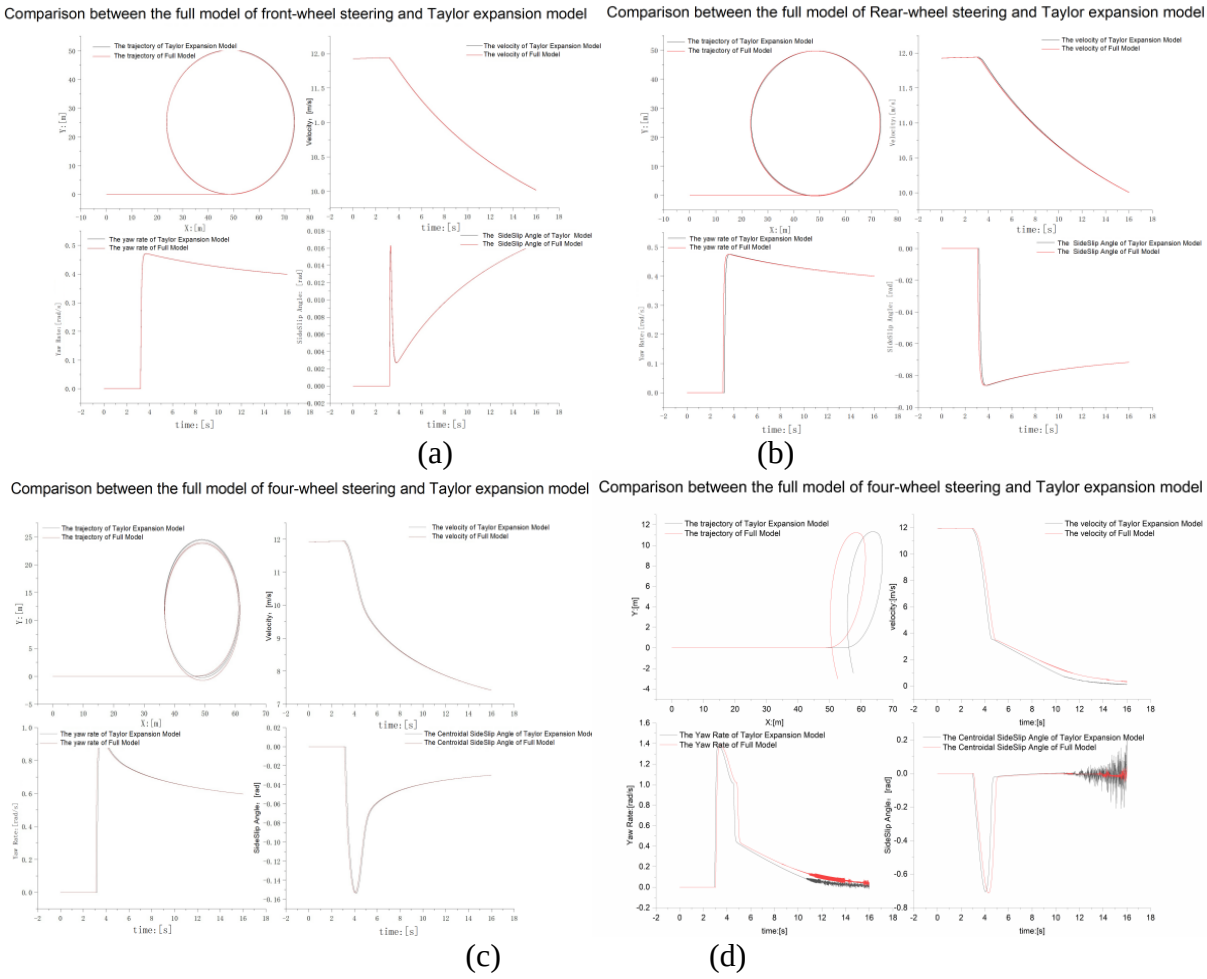

Figure 4: Comparison of Solutions between the Full Model and the simplified Model

(2) Comparison of Solution Spaces between the Full Model and the Two-Wheel Simplified Model

Here, the motor power of each wheel hub was also set at 1kW, with a desired torque of 10Nm, and the calculation step of the full model was set to 0.005s. Initially, the vehicle was allowed to drive straight until it reached a stable state, and then a step input was given to the tire angles. Since the two-wheel model cannot be compared with scenarios where all four wheel angles are different, a total of three experiments were conducted, with the tire angles set to [5, 5, 0, 0], [0, 0, -5, -5], and [5, 10, -4, -11]. The final simulation results comparing the two-wheel simplified model and the full model are shown in Figure 5. As can be seen from Figures 5(a) and 5(b), the trajectories obtained by the full model and the simplified model differ little, with position deviations in the x and y directions less than 0.5m and deviations in the centroid speed less than 0.1m/s. However, as illustrated in Figure 5(c), when a steering angle control of [5, 10, -4, -11] is applied to the vehicle, the results calculated by the simplified model deviate more from those of the full model, with a trajectory deviation of approximately 1m and a centroid speed deviation of around 1m/s. Regarding scenarios where the four wheel angles differ significantly, the two-wheel model is not suitable. It can be seen that the two-wheel model can only be used for cases where the left and right steering angles differ slightly.

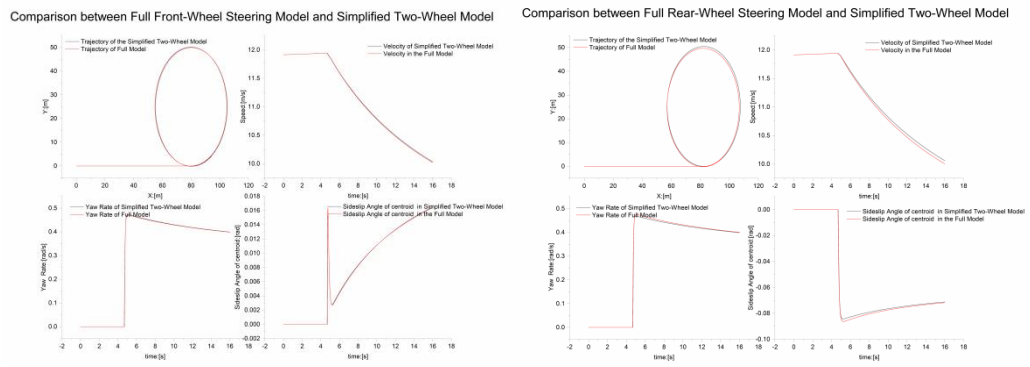

(a) (b)

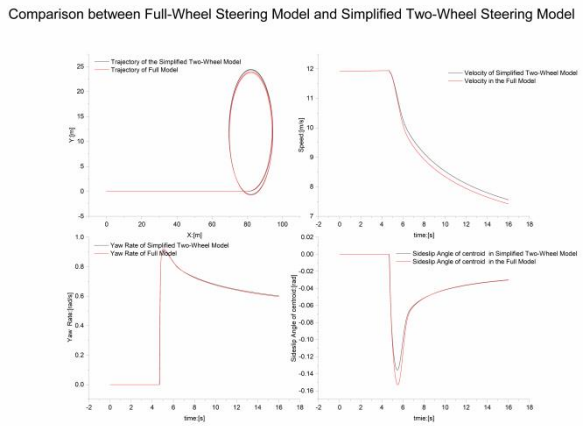

(c)

Figure 5: Comparison of Solutions between Two-Wheel Simplified Model and Taylor Series Expansion Model

(3) Comparison of the Full Model and the Simplified Model for the Yaw Angle of Centroid

For the simplified model that ignores the yaw angle of the centroid, the same motor power, torque, and calculation step as those used previously are employed. When the tire angles are set to [5, 5, 0, 0], [0, 0, -5, -5], [5, 5, -5, -5], and [5, 10, -4, -11], the results are shown in Figure 5. Since this model only ignores the yaw angle of the centroid, the calculations of other quantities remain the same in addition to final trajectories. Therefore, only the final trajectories are compared here. As shown in Figures 6(a) to 6(c), the trajectories calculated by the two models are identical for front-wheel steering, rear-wheel steering, and four-wheel steering models with small differences in yaw angles. However, when a steering angle control of [5, 10, -4, -11] is applied to the wheels, as shown in Figure 6(d), a deviation of about 5m in the x-direction of the final trajectory is observed. In this case, the yaw angles of the centroid cannot be ignored, or the final trajectory will have a significant deviation.

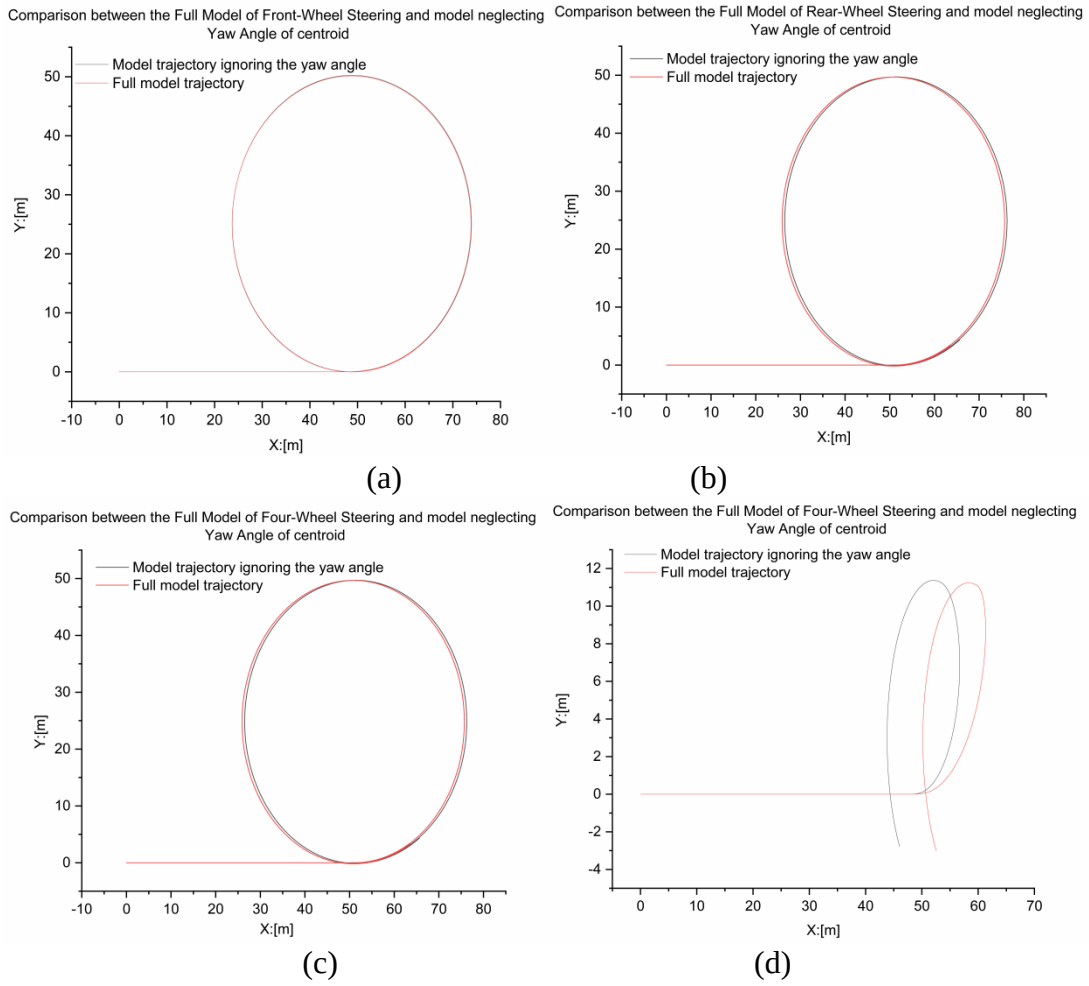

Figure 6: Comparison of Solutions between the Model Ignoring Yaw Angle of Centroid and Taylor Series Expansion Model

6. Conclusion

1) This paper establishes a 4WID-4WIS vehicle full model based on the magic formula tire model. The establishment of the full model is the foundation for solving and simplifying the model, and this paper also provides a numerical solution algorithm for this model.

2) This paper simplifies the model based on the magic formula tire model. Following the idea of simplifying the intermediate variables, the nonlinear implicit differential equations are reduced to discrete explicit differential equations. Simulation results prove that when the model is within the applicable range, the final solution of the simplified model is not significantly different from the results of the full model, and the results of the simplified model can be used to replace the results of the full model.

3) This paper derives a two-wheel model with five degrees of freedom based on the simplification of the full model. The simulation results of this model show slight differences from the solution of the full model. When the control applied to the vehicle's tires differs significantly, this simplified model cannot be used anymore, and the full model should be used for solving. For issues such as path planning and trajectory tracking for 4WID-4WIS vehicles, where the model can be simplified without requiring high solution accuracy, this simplified model can be used.

4) This paper also compares full model with a simplified model that ignores yaw angle of center

of mass. For the simplified model, its solution results are approximately the same as simulation results of full model. However, when the yaw angle is large, yaw angle cannot be directly ignored, and the error of the results derived from the simplified model will significantly increase. In such cases, the results calculated by the simplified model cannot replace the results calculated by the full model.

References

[1] Pacejka, H.B.; Bakker, E. The magic formula tyre model. Veh. Syst. Dyn. 1992, 21, 1-18.

[2] Solea R, Filipescu A, Filipescu S, et al. Sliding-mode controller for four-wheel-steering vehicle: Trajectory-tracking problem[C]//2010 8th World Congress on Intelligent Control and Automation. IEEE, 2010: 1185-1190.

[3] Maoqi L, Ishak M I, Heerwan P M. The effect of parallel steering of a four-wheel drive and four-wheel steer electric vehicle during spinning condition: a numerical simulation[C]//IOP Conference Series: Materials Science and Engineering. IOP Publishing, 2019, 469(1): 012084.

[4] Shi K, Yuan X, He Q. Double-layer dynamic decoupling control system for the yaw stability of four wheel steering vehicle[J]. International Journal of Control, Automation and Systems, 2019, 17(5): 1255-1263.

[5] Chen T, Chen L, Xu X, et al. Simultaneous path following and lateral stability control of 4WD-4WS autonomous electric vehicles with actuator saturation[J]. Advances in Engineering Software, 2019, 128: 46-54.

[6] Liang Y, Li Y, Yu Y, et al. Integrated lateral control for 4WID/4WIS vehicle in high-speed condition considering the magnitude of steering[J]. Vehicle System Dynamics, 2020, 58(11): 1711-1735.

[7] Liu Y, Zong C, Zhang D, et al. Fault-tolerant control approach based on constraint control allocation for 4WIS/4WID vehicles[J]. Proceedings of the Institution of Mechanical Engineers, Part D: Journal of Automobile Engineering, 2021: 0954407020982838.

[8] Hang P, Luo F, Fang S, et al. Path tracking control of a four-wheel-independent-steering electric vehicle based on model predictive control[C]//2017 36th Chinese Control Conference (CCC). IEEE, 2017: 9360-9366.

[9] Fahimi F. Full drive-by-wire dynamic control for four-wheel-steer all-wheel-drive vehicles[J]. Vehicle System Dynamics, 2013, 51(3): 360-376.

[10] Iervolino R, Sakhnevych A. Modeling, Simulation and Control of a 4WD Electric Vehicle with In-Wheel Motors[C]//International Conference on Robotics in Alpe-Adria Danube Region. Springer, Cham, 2017: 444-455.

[11] Hang P, Xia X, Chen X. Handling Stability Advancement with 4WS and DYC Coordinated Control: A Gain-scheduled Robust Control Approach[J]. IEEE Transactions on Vehicular Technology, 2021.

[12] Hang Peng, Chen Xinbo, Zhang Bang, et al. Active Path Planning and Tracking Control for Four-Wheel Independent Steering and Driving Electric Vehicles. Journal of Automotive Engineering, 2019, v.41; No.295(02):54-60